Blood in the Brain on Susceptibility-Weighted Imaging

Neeraj Jain[1] Sunil Kumar[1] Anuradha Singh[1] Shweta Jain[2] Rajendra Vishnu Phadke[1]

[1] Department of Radio Diagnosis, Sanjay Gandhi Postgraduate Institute of Medical Sciences, Lucknow, Uttar Pradesh, India
[2] Department of Pathology, Sanjay Gandhi Postgraduate Institute of Medical Sciences, Lucknow, Uttar Pradesh, India

Address for correspondence Neeraj Jain, DMRD, DNB, Department of Radio Diagnosis, Sanjay Gandhi Postgraduate Institute of Medical Sciences, Raebareli Road, Lucknow 226014, Uttar Pradesh, India (e-mail: neerajdmrd@gmail.com).

Indian J Radiol Imaging 2023;33:89–97.

Abstract

Intraparenchymal brain hemorrhage is not uncommon and results from a wide variety of causes ranging from trauma to tumor. Many a time, it is not possible to determine the exact cause of non-traumatic hemorrhage on conventional magnetic resonance imaging (MRI). Susceptibility-weighted imaging (SWI) is a high-resolution (3D) gradient-echo sequence. It is extremely sensitive to the inhomogeneity of the local magnetic field and highly useful in identifying the small amount of hemorrhage, which may be inapparent on other MR pulse sequences. In this review, we present different pattern of an intra-parenchymal brain hemorrhage on SWI with emphasis on differential diagnosis.

Keywords

- susceptibility-weighted imaging
- hemorrhage
- microhemorrhage
- brain hemorrhage
- magnetic resonance imaging

Introduction

Intraparenchymal brain hemorrhage is a frequently detected finding in magnetic resonance imaging (MRI) examination. Extensive parenchymal hemorrhages resulting from stroke and other causes are obvious on routine MRI sequences. However, difficulty arises in diagnosing microhemorrhages, which is a commonly associated finding with a wide variety of infective and noninfective conditions and may remain occult on conventional MRI sequences. Susceptibility-weighted MRI (SWI) sequence being sensitive to inhomogeneity of the local magnetic field can easily detect microhemorrhages, hence, offer added advantage over conventional MRI sequences.

SWI is a high-resolution 3D gradient-echo MRI sequence, which accentuates the difference between paramagnetic substances (e.g., deoxyhemoglobin, hemosiderin, and ferritin) and brain parenchyma, thereby making this sequence sensitive to detect even microhemorrhages. Moreover, it also contains inherent phase information, which is utilized in various MRI based flow-quantification (e.g., CSF flow, flow velocity in vessels). A typical SWI sequence yields four sets of images—magnitude, filtered phase, mIP (minimum intensity projection), and SW (susceptibility-weighted) image (►**Fig. 1**). The SWI is generated by creating a phase mask by combining the magnitude and phase images. To improve contrast to noise ratio, multiplication of the phase mask with the original magnitude image is done, which yields the final SWI image. The mIP image is generated by processing images with a 3 to 10 mm slice thickness and applying a minimum intensity projection algorithm. Paramagnetic substances such as hemosiderin, deoxyhemoglobin, and ferritin appear dark on magnitude images and bright on phase images on a left-handed MRI system relative to surrounding brain parenchyma. In contrast, diamagnetic substances such as calcium produce a negative shift and appear dark on phase images on left-handed MRI system.[1–3] On right-handed system, the deoxygenated blood will appear dark (negative phase) on phase images in relation to the surrounding tissue and calcium will look bright (positive phase) because calcium is diamagnetic relative to the brain tissue.[4]

article published online
December 7, 2022

DOI https://doi.org/10.1055/s-0042-1758880.
ISSN 0971-3026.

Thieme Medical and Scientific Publishers Pvt. Ltd., A-12, 2nd Floor, Sector 2, Noida-201301 UP, India

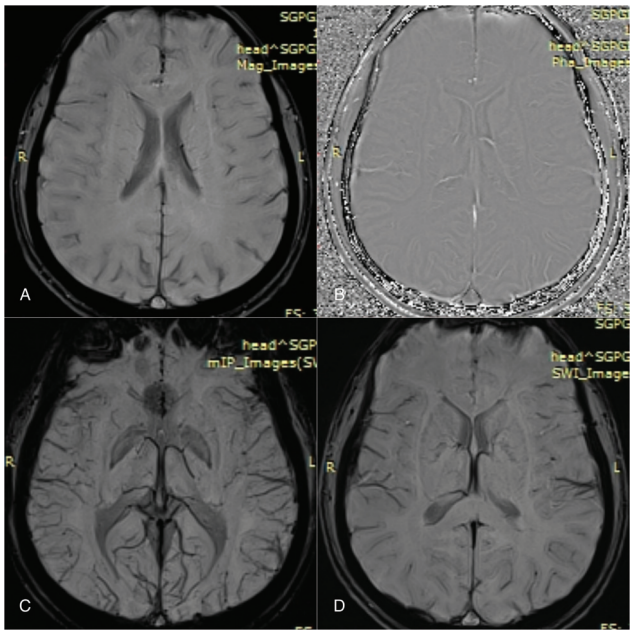

Fig. 1 Typical susceptibility-weighted imaging sequence, (**A**) magnitude images, (**B**) phase image, (**C**) mIP image, (**D**) susceptibility-weighted image.

Despite these, ferrocalcinosis is a condition where SWI may provide confusing signal intensity patterns as even basal ganglia "calcification" is often a mixture of paramagnetic iron and diamagnetic calcium. Yamada et al demonstrated that all basal ganglia calcifications show a paramagnetic susceptibility effect, whereas other calcifications located outside the basal ganglia (such as choroid plexus or dural calcifications) exhibit exclusively a diamagnetic susceptibility effect.[5]

Another issue with SWI imaging is problem of dipole artifact, which is due to imperfect diploic inversion of paramagnetic susceptibility. This artifact seen with bleed equal and/or larger than 3 mm. In left-handed system the upper and lower slices of hematomas will show hyperintense signal, while a right-handed system will show the opposite hypointense signal on the phase images. The stages of intracranial hemorrhage are hyperacute, acute, late subacute, and chronic. The differentiation between different stages could be achieved with the combination of T1, T2, and SWI images. Ideally, the evolution of intracranial bleed should result in higher susceptibility, and resultant increase signal on sequential signal-phase images. However, the inhomogeneous distribution of blood products often results in heterogeneous mixed hyper-, iso-, and hypo-signal intensities in the acute and early subacute stages. In the late subacute stage, the signal intensity on phase images will be more homogenous corresponding to the homogeneity in the extracellular distribution of methemoglobin. In contrast, chronic bleed will appear as volume loss of the affected cerebral parenchyma surrounded by hemosiderin staining.[6]

The intracranial bleed appears hyperintense on T1 during the late subacute stage, which is due to shortening of T1 relaxation time much more than T2 relaxation. This same mechanism explains the hyperintense signal produced by blood products on SWI at times. Although intracellular methemoglobin in early subacute hemorrhage also shortens T1 due to proton-electron dipole–dipole interactions, it is prone to susceptibility effects and appear hypointense on SWI, while extracellular methemoglobin in late subacute hemorrhage is not prone to significant susceptibility effects, allowing it to appear hyperintense on SWI.[7]

Scheid et al in their comparative analysis of 1.5 and 3 Tesla MRI for the evaluation of traumatic microbleeds found approximately two-fold increase in the total number of microbleeds on the 3T MRI system due to superior T2*-weighted gradient echo MRI at high field strengths. However, despite the heightened sensitivity of 3 T MRI, the vast majority of cases of probable diffuse axonal injury can be diagnosed by routine MRI at 1.5 T.[8]

Intraparenchymal hemorrhages are broadly divided into two subtypes—macrohemorrhage (>10 mm) and microhemorrhage (5–10 mm).

Cerebral Macrohemorrhages or Macrobleeds

Cerebral macrohemorrhages or macrobleeds are defined as bleed of more than 10 mm in size and commonly visible on conventional MRI sequences. Cerebrovascular pathologies such as hypertensive vasculopathy, cerebral amyloid angiopathy are the common non-traumatic causes of macrobleeds. Other causes are anticoagulant medications, vascular malformations, and aneurysmal rupture.

Cerebral Microhemorrhages or Microbleeds

Cerebral microhemorrhages or microbleeds are small foci of marked loss of signal intensity on T2*-weighted or SWI. The majority of studies define microhemorrhages as being smaller than 5 mm in diameter with an upper limit of 10 mm. However, recent studies have suggested that the size also depends upon magnetic field strength and pulse sequence.[9] Likewise, no separate consensus definition of more fine hemorrhages had been developed.

For the ease of differentiation, we proposed to divide bleed smaller than 10 mm size into two categories—microbleed or microhemorrhage (5–10 mm) and petechial hemorrhage (<5 mm).

Microbleeds

Cerebral microbleeds are more common in older individuals as a part of aging. However, several other diseases such as Alzheimer's dementia, chronic hypertensive encephalopathy, cerebral amyloid angiopathy, cerebral autosomal dominant arteriopathy with subcortical infarcts and leukoencephalopathy (CADASIL), radiation therapy and trauma also reveal microbleeds.[10,11]

Petechial Hemorrhage

Diffuse petechial hemorrhages are commonly detected in various infectious conditions, which may or may not be associated with thrombocytopenia such as malaria, dengue, scrub typhus, and idiopathic thrombocytopenic purpura.

Table 1 Causes and distribution of various types of hemorrhages (CADASIL-cerebral autosomal dominant arterio-pathy with subcortical infarcts and leukoencephalopathy, PRES-posterior reversible encephalopathy syndrome, PACNS-primary angiitis of central nervous system)

Central Hemorrhage		**Peripheral Hemorrhage**	
Micro	**Macro**	**Micro**	**Petechial**
Hypertension	Hypertension	CADASIL	Cerebral Malaria
Amyloid angiopathy	Sinus Thrombosis	Vasculitis	Scrub Typhus
Encephalitis	Japanese Encephalitis	Dengue	Viral Encephalitis
	H1N1 Encephalitis	Hypertension	PRES
		PACNS	

Linear or Streaky Hemorrhage

Linear or streaky hemorrhage are commonly seen in subarachnoid hemorrhage (SAH) and vasculitis such as primary CNS angiitis. In vasculitis, it may be either due to vascular/perivascular inflammation or SAH.

Depending on the site of involvement, two distinct types of intraparenchymal hemorrhage are central and peripheral. The central type affects thalamus, brain stem, and basal ganglia, while peripheral type involves cerebral and cerebellar cortical and subcortical regions. However, wide overlap exists as various conditions involve both peripheral and central parts such as CADASIL, hypertensive encephalopathy, and viral encephalitis (►**Table 1**).

In this review, we would be discussing the various causes of cerebral bleeds such as infection, vasculitis, or other miscellaneous etiologies with an emphasis on the pattern of blooming on SWI.

Infections

Cerebral Malaria

It is a fatal neurological complication of *Plasmodium* infection particularly associated with *Plasmodium falciparum*. The plugging of small-caliber blood vessels by *Plasmodium* may result in intracranial hemorrhage. Malaria should be suspected in cases with acute-onset fever with associated chills and rigors in endemic regions. Drowsiness may suggest cerebral involvement MRI in cerebral malaria demonstrates diffuse petechial hemorrhages throughout the cerebral hemisphere in peripheral distribution, predominantly at the gray–white matter junction. SWI is extremely useful in the detection of these diffuse petechial hemorrhages. Besides, involvement of the corpus callosum is quite common and characteristic of this entity, which appears hyperintense on T2/FLAIR due to white matter edema and may also have petechial hemorrhages as well (►**Figs. 2**, **3**).[12]

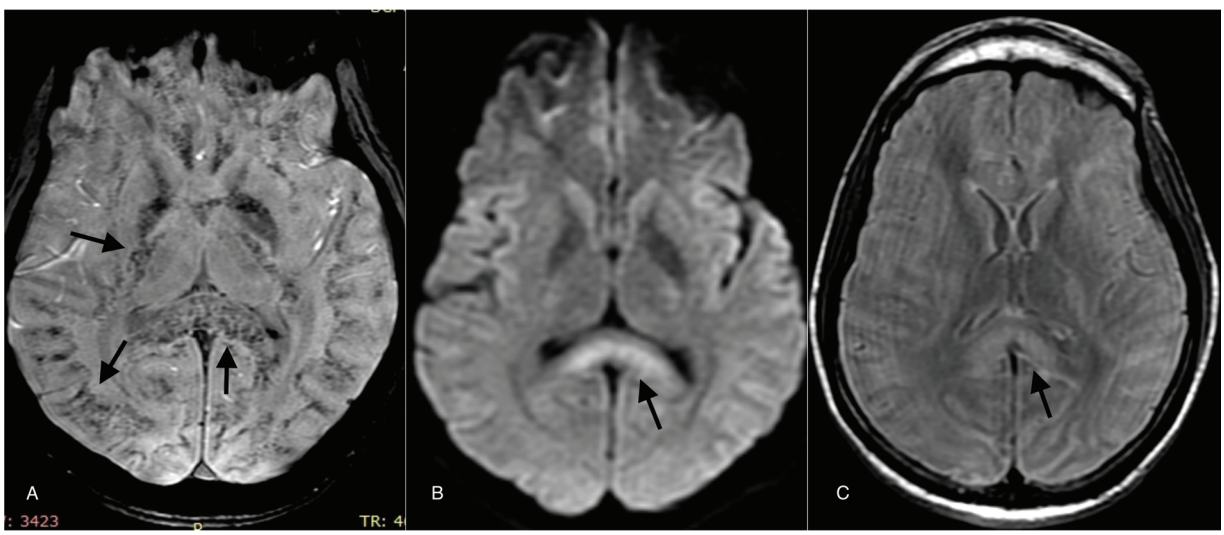

Fig. 2 Cerebral malaria, axial SWI image (**A**) shows diffuse petechial hemorrhages in bilateral fronto-temporo-parietal regions, internal and external capsule and splenium of the corpus callosum. Axial DWI images (**B**) shows hyperintense signal in the splenium of corpus callosum, axial FLAIR image (**C**) shows hyperintense signal bilateral cerebral hemispheres in the cortical-subcortical region and also in the splenium of corpus callosum. However, both DWI and FLAIR images fail to demonstrate petechial hemorrhages (Malarial parasites were detected on microscopic examination of peripheral blood smear).

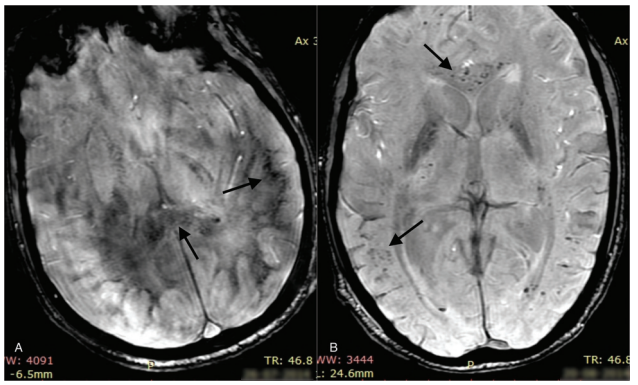

Fig. 3 Cerebral malaria, axial SWI images (**A** and **B**) in two different patients shows diffuse petechial hemorrhages in bilateral cerebral hemispheres with the involvement of corpus callosum (malarial parasites were detected on microscopic examination of peripheral blood smear).

Dengue

Dengue is a febrile viral illness, transmitted by *Aedes* mosquito. The causative agent is a dengue virus, an arbovirus RNA virus, belonging to the Flaviviridae family with four serotypes (NS1–NS4) known. Although considered a non-neurotropic virus, neurological manifestations may rarely (4–5% of cases) be seen with NS2 and NS3. These complications are usually an immune-mediated phenomenon that may lead to acute demyelinating encephalomyelitis (ADEM), Guillain–Barre syndrome (GBS), neuritis, myelitis, hypokalemic paralysis, and opsoclonus myoclonus.

Hemorrhagic fever is a severe complication of dengue fever. It can result in severe thrombocytopenia and coagulopathy, which can result in intracranial hemorrhage, if left untreated. Dengue hemorrhagic encephalitis is, in fact, a hemorrhagic variant of ADEM, a severe form with a rapid downhill course.

Imaging findings may be normal or may show various types of intracranial hemorrhage (parenchymal, subarachnoid, subdural, or extradural) occurring due to thrombocytopenia or from increased vascular permeability. The hemorrhages are usually larger than those of malaria, and sometimes large intraparenchymal hematoma is also seen. Various studies have shown frequent involvement of brain parenchyma with features of diffuse cerebral edema and signal alteration in the deep gray nuclei. In fact, signal alteration in the basal ganglia–thalamus complex is the most common abnormality on MRI. This leads to symmetrical T2/FLAIR hyperintensity in the thalami and pones. Additionally, there may be signal abnormalities in the medial temporal lobe, midbrain, or cerebellum. These may have diffusion restriction and post-contrast enhancement. Multiple blooming foci suggestive of microhemorrhages may be seen within the affected areas. These microhemorrhages are most likely due to perivenular inflammation and demyelination resulting from immune-mediated necrotizing vasculitis of venules. These portend a poor prognosis and may lead to cognitive and other functional impairments in survivors.[13,14]

In endemic regions, dengue hemorrhagic fever (DHF) usually spreads post-Monsoon season, corresponding to increased mosquito breeding due to water logging. Onset is acute with fever, bone, and retro-orbital pain and may be associated with petechial rash. The presence of multiple microhemorrhages in the brain increases the likelihood of DHF (►**Fig. 4**) as similar imaging findings may be seen in other viruses of the Flaviviridae family such as Japanese encephalitis and West Nile virus. However, the timeline of seasonal variation coupled with endemicity is a clue to the diagnosis.

Scrub Typhus

Scrub typhus is an acute febrile illness caused by gram-negative bacteria, *Orientia tsutsugamushi*, which is transmitted by trombiculid mites. It can involve multiple organs, including the central nervous system. Because of associated vasculitis and perivasculitis, it may result in intracranial hemorrhage. Similar to many other viral illnesses, thrombocytopenia is a frequent finding, which in addition to vasculitis and encephalitis can also contribute to the development of intracranial hemorrhages.

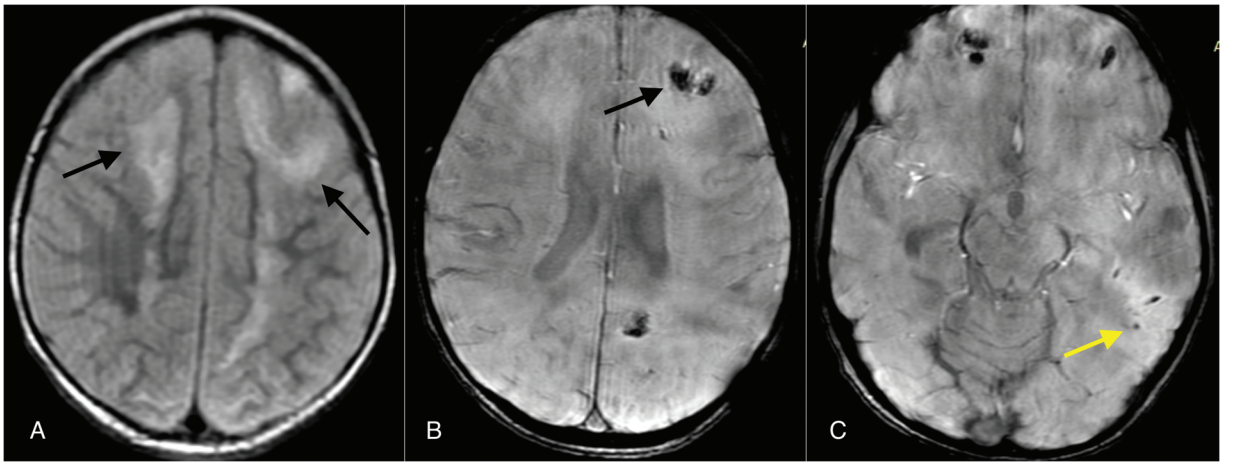

Fig. 4 Dengue hemorrhagic fever, Axial FLAIR image (**A**) shows symmetrical hyperintense signal in bilateral frontoparietal white matter and right frontal gray matter. Axial SWI images (**B, C**) show multiple macrobleeds and microbleeds in bilateral frontal and left parietal posterior temporal lobe. (Diagnosis was confirmed by positive dengue serology).

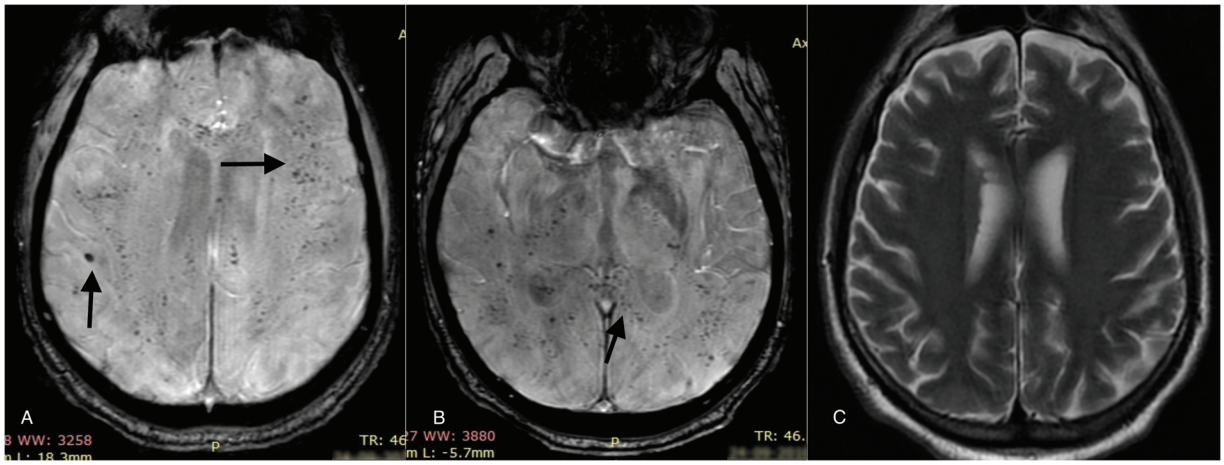

Fig. 5 Scrub typhus, axial SWI images (**A, B**) shows diffuse petechial and few microhemorrhages in bilateral cerebral hemispheres also involving internal capsule and corpus callosum. Axial T2 images (**C**) appear essentially normal (diagnosis was confirmed by positive scrub typhus serology).

Diffuse petechial hemorrhages are the frequently reported in scrub typhus. However, other MRI findings such as meningoencephalitis/encephalopathy, T2/FLAIR hyperintensities in white matter, and microhemorrhages may also present (►**Fig. 5**).The affected regions may show restricted diffusion. Imaging findings involving subcortical white matter may be indistinguishable from posterior reversible encephalopathy syndrome (*vide infra*). However, febrile presentation in an endemic region favors the diagnosis of Scrub typhus. The diagnosis of scrub typhus is confirmed by demonstrating raised antibody titer by Weil–Felix agglutination test or indirect immunofluorescence test.[15–17]

H1N1 Encephalitis

H1NI virus, which is a novel influenza A virus may involve cerebral parenchyma. The spectrum of neurological manifestations in H1N1 encephalitis vary from acute necrotizing encephalopathy, encephalitis, meningitis/meningoencephalitis, and opportunistic fungal infection. Acute necrotizing encephalitis is a fulminant condition, which is characterized by bilateral symmetric involvement of thalamus with the hyperintense signal on T2/FLAIR sequences and restricted diffusion. Other regions such as basal ganglia, brainstem, cerebellum, and periventricular white matter may also be involved. Neuronal and glial necrosis characteristically leads to peripheral diffusion restriction. These lesions are frequently associated with microbleeds/petechial bleeds. SWI is a useful technique in the detection and better characterization of the extent of hemorrhage, which may be inapparent on other MR pulse sequences (►**Fig. 6**). Meningoencephalitis may involve subcortical white matter in frontal and parietal lobes, bilateral thalami, and corpus callosum. Some case reports also suggest the involvement of the perirolandic region with leptomeningeal enhancement.[18–20]

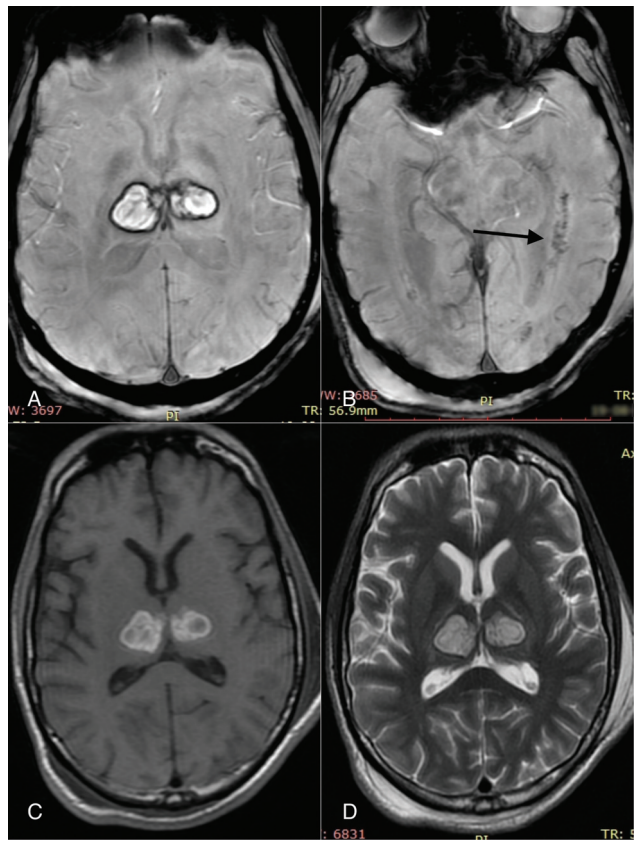

Fig. 6 H1N1 encephalitis, axial SWI image (**A**) shows symmetrical hyperintense areas in bilateral thalamus with a peripheral rim of a dark signal representing hemosiderin, axial SWI image (**B**) shows petechial hemorrhages in the left parieto-temporal region along the left lateral ventricle (arrow). Axial T1 (**C**) and T2 (**D**) images show same areas showing hyperintense signal on both T1 and T2 weighted images representing late subacute hemorrhage (diagnosis was confirmed by positive H1N1 serology).

Primary Angiitis of Central Nervous System

Primary angiitis of central nervous system (PACNS) is a single organ vasculitis exclusive to the CNS in the absence of any systemic involvement. It is a medium- to small-vessel vasculitis, usually affecting the individuals of 40 to 50 years age group. The inflammation of the blood vessel wall with resultant stenosis and obstruction of the vessel lumen is a predominant pathology behind the development of intracranial hemorrhage.

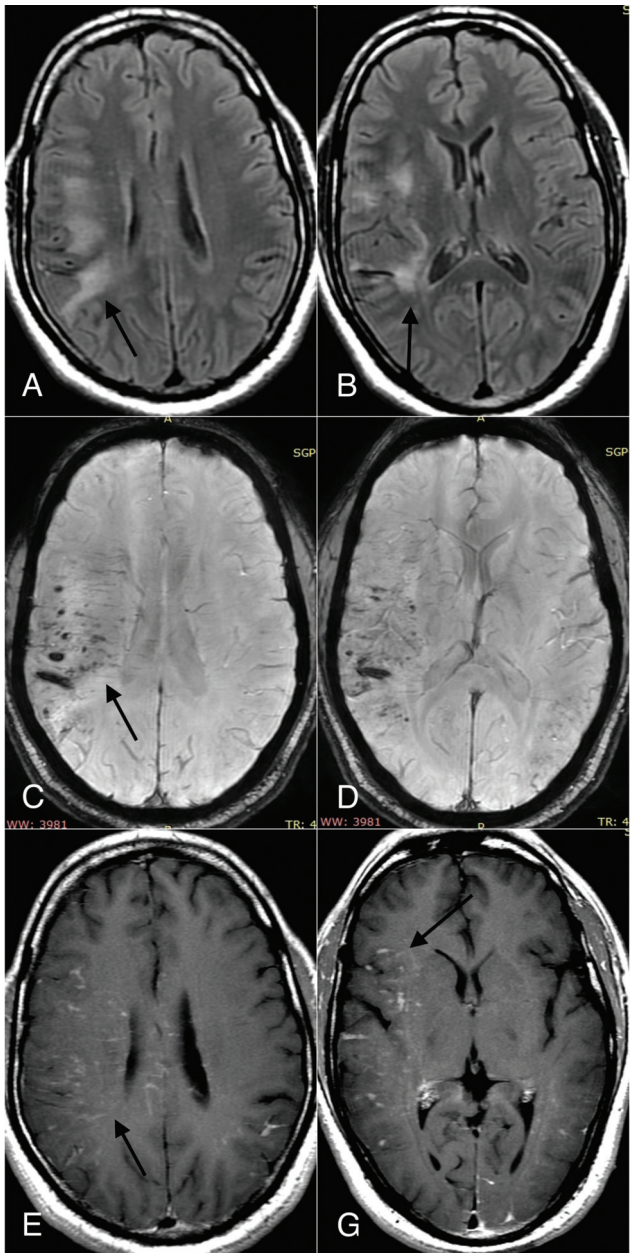

Fig. 7 Case of primary angiitis of the central nervous system, axial FLAIR images (**A, B**) abnormal areas with the hyperintense signal in right temporoparietal region predominantly involving subcortical white matter. Axial SWI images (**C, D**) show multiple microhemorrhages and linear streaky peri-vascular hemorrhages in involved areas. Axial contrast images (**E, F**) shows multiple linear and punctate enhancement in the right frontoparietal and left parietal region (diagnosis confirmed at brain biopsy).

MR findings are nonspecific, which include infarcts, white matter lesions, and confluent lesions with a pseudo-mass-like appearance mimicking demyelination or even neoplasm. MR angiography may demonstrate vascular abnormalities in large and medium vessel vasculitis. Small vessel vasculitis, in contrast, may have no abnormality on conventional MRI, the diagnosis of which may be suspected only by a demonstration of microbleeds on gradient-echo images. SWI better demonstrates the extent of hemorrhagic lesions and also

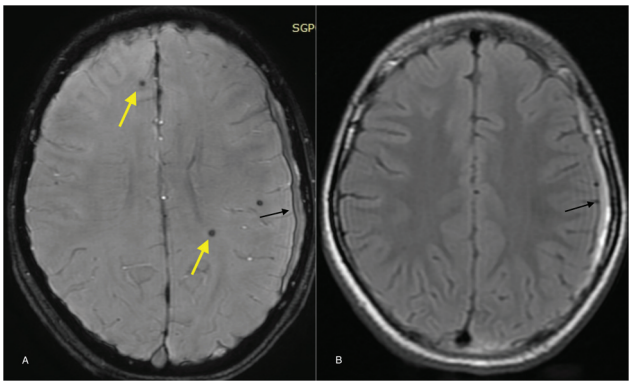

Fig. 8 Idiopathic thrombocytopenic purpura axial SWI image (**A**) shows multiple microhemorrhages in bilateral frontal lobes and left subdural hematoma (arrow). Axial FLAIR image (**B**) fails to demonstrate microhemorrhage, however, left subdural hematoma is seen (arrow). (diagnosis confirmed at bone marrow study).

reveals inapparent subarachnoid hemorrhage, parenchymal, and microhemorrhages.[21–24]

This entity should be suspected in middle-aged individuals presenting with history of headache and recurrent stroke-like symptoms. MRI findings of recurrent bleed with multiple linear/streaky perivascular blooming with adjacent T2/FLAIR hyperintensity and linear/punctate or lace-like enhancement, is highly suggestive of PACNS (►**Fig. 7**). Linear or lace-like blooming with irregular margins in PACNS is attributed histopathologically to perivenular inflammation with leucocytic infiltration in Virchow–Robin spaces. Lace-like enhancement in the adjacent parenchyma may be suggestive of contrast extravasation secondary to the breach in the blood–brain barrier.

Miscellaneous

Idiopathic Thrombocytopenic Purpura

The most common cause of cerebral microbleeds is age-related macroangiopathy, which gets exacerbated by risk factors such as hypertension followed by amyloid angiopathy. Besides these, other causes of cerebral microbleeds are cerebral small vessel diseases, including both familial amyloid and nonamyloid angiopathies and hematological disorders.

Idiopathic thrombocytopenic purpura (ITP) is an autoimmune hematological disorder characterized by increased destruction of platelets in the reticuloendothelial system. Marked thrombocytopenia can result in clinically apparent intracranial hemorrhage, which may be intraparenchymal, intraventricular, or subdural. The presence of various types of hemorrhages such as microbleeds, intraparenchymal hematoma, and the subdural hematoma in a single MRI scan should prompt the search for this entity or other coagulopathies (►**Fig. 8**).

Nonetheless, even asymptomatic patients may have occult microhemorrhages, which may be better detected by SWI. Such microhemorrhages may be a harbinger of future macro-hemorrhagic events in such patients, thereby identifying the at-risk population.[25–27]

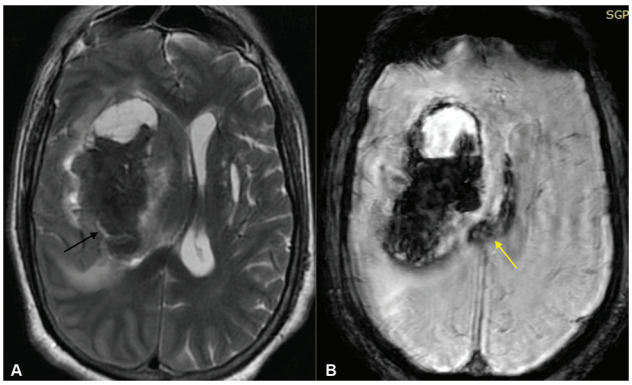

Fig. 9 Case of acute hypertensive bleed, axial T2 image (**A**) shows a fairly large area of hypointense signal centered on right ganglia-thalamic region causing mass effect over right lateral ventricle. Axial SWI image (**B**) demonstrate "blooming" with the extension of bleed in lateral ventricle, which is not very much apparent on T2 image.

Hypertensive Microangiopathy and Hypertensive Intracerebral Hemorrhage

Acute hypertensive bleed frequently occurred in the central part of the brain, i.e., basal ganglia thalamus and brain stem. However, there may be involvement of the cerebral and cerebellar hemispheres as well.

Microbleeds are the reasonably common manifestation of chronic hypertensive encephalopathy, which is often missed on the conventional MRI sequences. SWI being sensitive sequences to paramagnetic substances can very well demonstrate the extension of acute intracranial bleed as well as microbleeds of chronic hypertensive encephalopathy, predominantly involving the basal ganglia, thalamus, and brainstem (►**Figs. 9**, **10**).[28]

Posterior Reversible Encephalopathy Syndrome

Posterior reversible encephalopathy syndrome (PRES) is a clinico-radiological syndrome, resulting from accelerated blood pressure that exceeds the auto-regulatory capacity of the brain vasculature. This syndrome also associated with preeclampsia/eclampsia, renal decompensation, and immunosuppressive drugs.

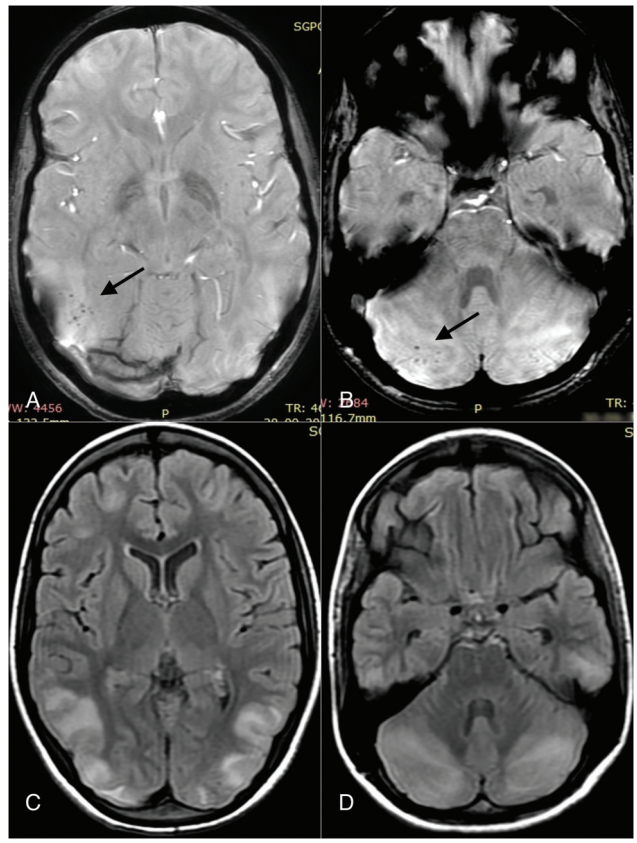

Fig. 11 Posterior reversible encephalopathy, axial SWI images (**A, B**) show multiple petechial hemorrhages in right posterior temporal and bilateral cerebellar hemispheres posteriorly (arrows). Axial FLAIR images (**C, D**) show symmetrical abnormal hyperintense signal bilateral posterior temporal, parietal and cerebellar hemispheres.

MRI findings in typical cases are fairly characteristic with bilateral symmetrical T2/FLAIR hyperintensity in the region supplied by posterior circulation, e.g., parietal, occipital, posterior temporal, and cerebellar hemispheres. Atypical imaging findings include the presence of hemorrhage,

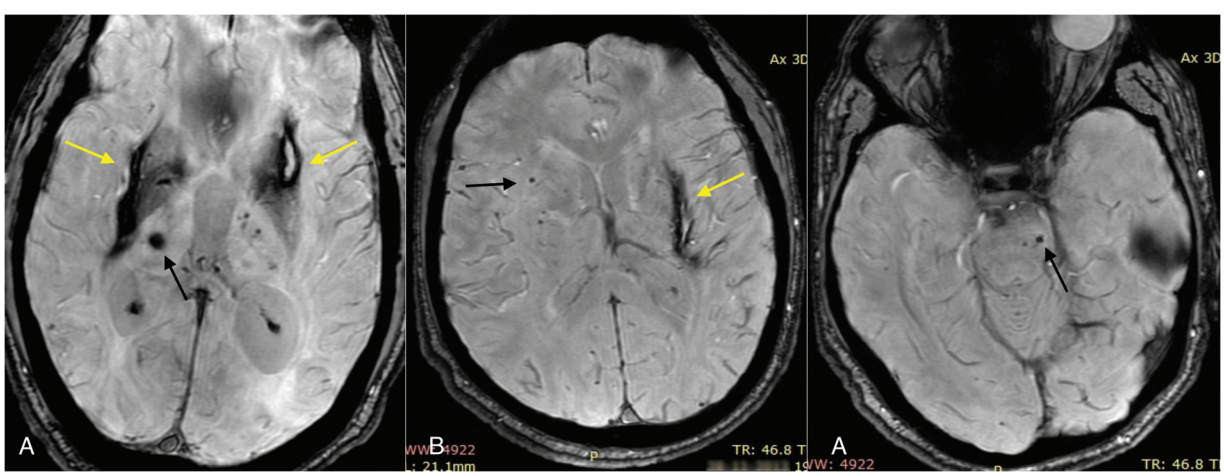

Fig. 10 Chronic hypertensive encephalopathy, axial SWI image (**A**) shows multiple micro-hemorrhages centered on bilateral thalamus (black arrow) with macro- hemorrhages in bilateral basal ganglia (yellow arrows). Axial SWI images (**B, C**) in a different patient show micro-hemorrhages in right basal ganglia and brain stem (black arrows) and old macro-hemorrhage in left basal ganglia.

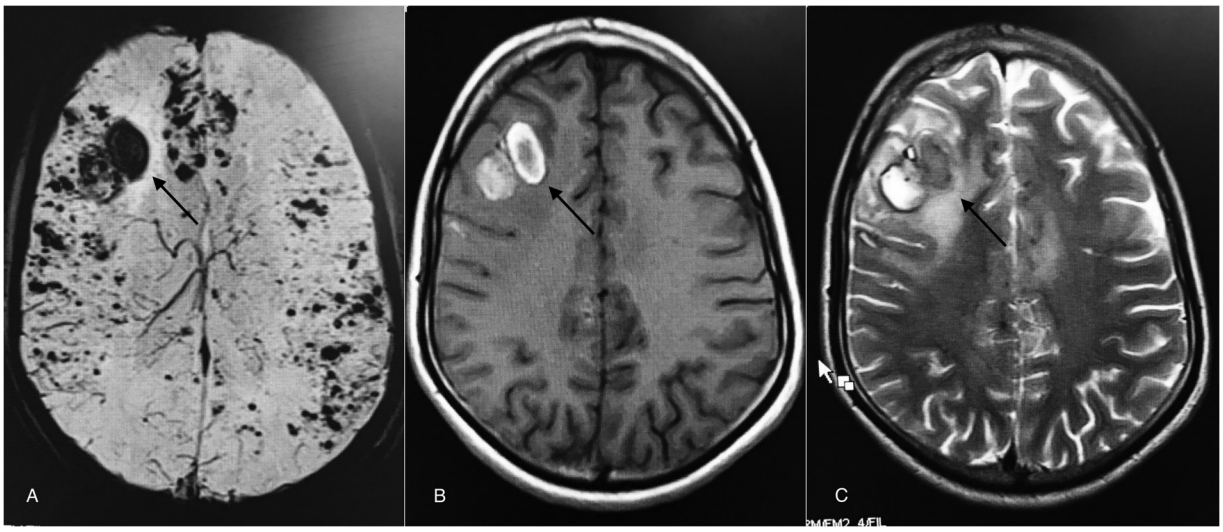

Fig. 12 Cerebral amyloid angiopathy, axial SWI image shows (**A**) large macrobleed in the right frontal region (arrow) with extensive microbleeds in bilateral cerebral hemispheres. Axial T1 (**B**) and T2 (**C**) images show clearly shows a late subacute macrobleed in the right frontal lobe, however, except a few microbleeds which are clearly seen on SWI image are not seen.

diffusion restriction or contrast enhancement. Intracranial hemorrhage is not uncommon, seen in around 15% of cases, which include microhemorrhages, subarachnoid hemorrhage, and focal hematoma (►**Fig. 11**).[21,29]

Cerebral Amyloid Angiopathy (CAA)

Amyloid angiopathy is a small vessel disease that occurs due to the deposition of β-amyloid in the vessel wall. Cerebral amyloid angiopathy (CAA) is an age-related disorder with a prevalence of 75% in patients aged 90 years or older and also associated with aging, dementia, and Alzheimer's disease.

Intracranial hemorrhage in CAA commonly manifests as microbleeds centering on the cortical-subcortical junction with lobar and cortical siderosis. The microbleeds predominantly affect the peripheral part of the brain (►**Fig. 12**).[3,21] Histopathologically, microbleeds result from damage to the elastic lamina of the arteries consequential to the amyloid deposition. The presence of superficial parenchymal hemorrhage involving both cortex–subcortical white matter, frontal and parietal lobes should raise the suspicion of CAA. Detection of microbleeds and their subsequent follow-up help in risk stratification for future hemorrhagic events besides monitoring therapeutic response.

Cerebral Autosomal Dominant Arteriopathy with Subcortical Infarcts and Leukoencephalopathy (CADASIL)

CADASIL is an autosomal dominant arteriopathy manifesting at 40 to 50 years of age . Recurrent transient ischemic attacks (TIAs), strokes in multiple vascular territories, and migraine are the most common presenting symptoms.

MRI shows bilateral symmetrical T2/FLAIR hyperintensity in the periventricular and deep white matter involving subinsular white matter, external capsule, frontal, and anterior temporal lobes. Superficial white matter is less commonly affected with relative sparing of the cerebral cortex and arcuate fibers. Lacunar infarcts and dilated

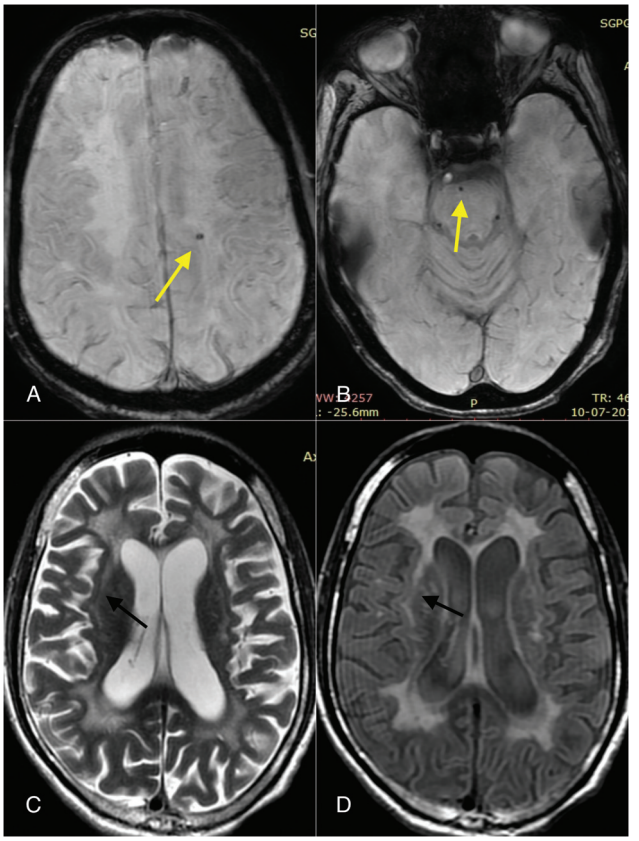

Fig. 13 Cerebral autosomal dominant arteriopathy with subcortical infarct and leukoencephalopathy, axial SWI images (**A, B**) show micro hemorrhage in left subcortical white matter and pons. Axial T2 (**C**) and FLAIR (**D**) images show symmetrical hyperintense signal in bilateral periventricular and subcortical white matter with typical involvement of subinsular region (arrow).

Virchow–Robin spaces at the gray–white matter junction and basal ganglia are also commonly seen. Microbleeds are the well-known features of this condition and seen in various parts of the brain with a preference for cortical-

subcortical regions. Cerebral white matter, thalamus, and brainstem are less frequently involved. However, Lesnik Oberstein et al found that thalamus is the most common site for microbleeds (►**Fig. 13**).[30] The typical location of microbleeds is outside the ischemic areas. These microbleeds may be present in both symptomatic as well as asymptomatic cases. These patients have a remote risk of intracranial hemorrhage of which cerebral microbleeds may be a predictor.[30,31]

The diagnosis of this condition based on characteristic MRI findings of white matter hyperintensities, lacunar infarcts, and cerebral microbleeds in an appropriate clinical backdrop. Confirmation is by the demonstration of NOTCH3 mutation on genetic analysis. The involvement of anterior temporal lobe helps in differentiating this entity from other small vessel arteriopathies.

Conclusion

SWI is a sensitive MRI sequence helpful in detecting brain hemorrhage and can also help in identifying the underlying cause or narrowing down the differential diagnosis based on various patterns.

Funding
None.

Conflict of Interest
None declared.

References

1 Haacke EM, Mittal S, Wu Z, Neelavalli J, Cheng YC. Susceptibility-weighted imaging: technical aspects and clinical applications, part 1. Am J Neuroradiol 2009;30(01):19–30
2 Chavhan GB, Babyn PS, Thomas B, Shroff MM, Haacke EM. Principles, techniques, and applications of T2*-based MR imaging and its special applications. Radiographics 2009;29(05):1433–1449
3 Mittal S, Wu Z, Neelavalli J, Haacke EM. Susceptibility-weighted imaging: technical aspects and clinical applications, part 2. Am J Neuroradiol 2009;30(02):232–252
4 Sood S, Gupta R, Modi J, Sharma J. Susceptibility weighted imaging: physics and clinical applications in neuroimaging at 3 Tesla. Conference Paper. March 2014. Doi: 10.1594/ecr2014/C-1472
5 Lee YJ, Lee S, Jang J, et al. Findings regarding an intracranial hemorrhage on the phase image of a susceptibility-weighted image (SWI), according to the stage, location, and size. Investig Magn Reson Imaging 2015;19(02):107–113
6 Zimmerman RD, Yousem DM, Grossman RI. Vascular diseases of the brain. Neuroradiology: the requisites. 3rd ed. St. Louis: Mosby; 2010:141–160
7 Yamada N, Imakita S, Sakuma T, Takamiya M. Intracranial calcification on gradient-echo phase image: depiction of diamagnetic susceptibility. Radiology 1996;198(01):171–178
8 Scheid R, Ott DV, Roth H, Schroeter ML, von Cramon DY. Comparative magnetic resonance imaging at 1.5 and 3 Tesla for the evaluation of traumatic microbleeds. J Neurotrauma 2007;24(12):1811–1816
9 Nandigam RN, Viswanathan A, Delgado P, et al. MR imaging detection of cerebral microbleeds: effect of susceptibility-weighted imaging, section thickness, and field strength. AJNR Am J Neuroradiol 2009;30(02):338–343
10 Blitstein MK, Tung GA. MRI of cerebral microhemorrhages. Am J Roentgenol 2007;189(03):720–725
11 Haller S, Vernooij MW, Kuijer JPA, Larsson EM, Jäger HR, Barkhof F. Cerebral microbleeds: imaging and clinical significance. Radiology 2018;287(01):11–28
12 Baliyan V, Nadarajah J, Kumar A, Ahmad Z. Cerebral malaria: susceptibility weighted MRI. Asian Pacific J Trop Dis 2015; 5:239–241
13 Soni BK, Das DSR, George RA, Aggarwal R, Sivasankar R. MRI features in dengue encephalitis: a case series in South Indian tertiary care hospital. Indian J Radiol Imaging 2017;27(02): 125–128
14 Jugpal TS, Dixit R, Garg A, et al. Spectrum of findings on magnetic resonance imaging of the brain in patients with neurological manifestations of dengue fever. Radiol Bras 2017;50(05):285–290
15 Jeong YJ, Kim S, Wook YD, Lee JW, Kim KI, Lee SH. Scrub typhus: clinical, pathologic, and imaging findings. Radiographics 2007;27 (01):161–172
16 Sood S, Sharma S, Khanna S. Role of advanced MRI brain sequences in diagnosing neurological complications of scrub typhus. J Clin Imaging Sci 2015;5:11
17 Neyaz Z, Bhattacharya V, Muzaffar N, Gurjar M. Brain MRI findings in a patient with scrub typhus infection. Neurol India 2016;64 (04):788–792
18 Zeng H, Quinet S, Huang W, et al. Clinical and MRI features of neurological complications after influenza A (H1N1) infection in critically ill children. Pediatr Radiol 2013;43(09):1182–1189
19 Gulati P, Saini L, Jawa A, Das CJ. MRI in H1N1 encephalitis. Indian J Pediatr 2013;80(02):157–159
20 Haktanir A. MR imaging in novel influenza A (H1N1)-associated meningoencephalitis. AJNR Am J Neuroradiol 2010;31(03): 394–395
21 Chen JJ, Carletti F, Young V, Mckean D, Quaghebeur G. MRI differential diagnosis of suspected multiple sclerosis. Clin Radiol 2016;71(09):815–827
22 Abdel Razek AA, Alvarez H, Bagg S, Refaat S, Castillo M. Imaging spectrum of CNS vasculitis. Radiographics 2014;34(04):873–894
23 Aviv RI, Benseler SM, Silverman ED, et al. MR imaging and angiography of primary CNS vasculitis of childhood. Am J Neuroradiol 2006;27(01):192–199
24 Singh S, John S, Joseph TP, Soloman T. Primary angiitis of the central nervous system: MRI features and clinical presentation. Australas Radiol 2003;47(02):127–134
25 Lee MS, Kim WC. Intracranial hemorrhage associated with idiopathic thrombocytopenic purpura: report of seven patients and a meta-analysis. Neurology 1998;50(04):1160–1163
26 Flores A, Buchanan GR. Occult hemorrhage in children with severe ITP. Am J Hematol 2016;91(03):287–290
27 Fazekas F, Kleinert R, Roob G, et al. Histopathologic analysis of foci of signal loss on gradient-echo T2*-weighted MR images in patients with spontaneous intracerebral hemorrhage: evidence of microangiopathy-related microbleeds. Am J Neuroradiol 1999; 20(04):637–642
28 Zafar A, Khan FS. Clinical and radiological features of intracerebral haemorrhage in hypertensive patients. J Pak Med Assoc 2008;58 (07):356–358
29 Hefzy HM, Bartynski WS, Boardman JF, Lacomis D. Hemorrhage in posterior reversible encephalopathy syndrome: imaging and clinical features. Am J Neuroradiol 2009;30(07):1371–1379
30 Lesnik Oberstein SAJ, van den Boom R, van Buchem MA, et al; Dutch CADASIL Research Group. Cerebral microbleeds in CADASIL. Neurology 2001;57(06):1066–1070
31 Dichgans M, Holtmannspötter M, Herzog J, Peters N, Bergmann M, Yousry TA. Cerebral microbleeds in CADASIL: a gradient-echo magnetic resonance imaging and autopsy study. Stroke 2002;33 (01):67–71

